Geophysical & Astrophysical Fluid Dynamics

Tidally induced mean flow over bathymetric features: a contemporary challenge for high-resolution wide-area models

Jeff A. Polton[a]

[a] National Oceanography Centre, Joseph Proudman Building, 6 Brownlow Street, Liverpool, L3 5DA, UK.
Published online: 23 Sep 2014.

CrossMark

Click for updates

PLEASE SCROLL DOWN FOR ARTICLE

Taylor & Francis
Taylor & Francis Group

Tidally induced mean flow over bathymetric features: a contemporary challenge for high-resolution wide-area models

JEFF A. POLTON*

National Oceanography Centre, Joseph Proudman Building, 6 Brownlow Street, Liverpool L3 5DA, UK

Huthnance [*Estuarine Coastal Mar. Sci.* 1973, **1**, 89–99] is reviewed, whereby an oscillating tide over bathymetric features induces a mean flow generally along isobaths. The effect is a superposition of Coriolis and frictional processes. These are discussed with the intention of elucidating the processes for a more general readership. Induced velocities of order several cm s^{-1} are expected around the UK shelf seas. The effect is dynamically significant over bathymetric scales of order a few kilometres and has previously been of most interest to dynamicists studying processes on this scale. However, with the increase in computing power, appropriate scales can be simulated in shelf-wide regional models and in next generation operational models. It is demonstrated that this small-scale effect is likely to be important for shelf-wide regional models and that a spatial resolution of at least 1.8 km is recommended for shelf sea simulations.

Keywords: Regional model; Resolution; Tides; Tidal residual; Bathymetry; Tidal excursion

1. Introduction

Huthnance (1973), "Tidal current asymmetries over the Norfolk Sandbanks", was motivated by some unexplained observations of mean flows along sandbanks (Caston and Stride 1970). These sandbanks were typically 40 km long by 2 km wide, of height 30 m in the shallow water of depth of 40 m and critically were present in the tidally active waters in the southern North Sea. The major axes of the tidal ellipses are not aligned with the long axis of the bathymetric features (figure 1) such that over a tidal period, water columns are forced up and down the bathymetric slopes. This asymmetry in the ebb and flood tides results in tidally induced mean currents (herein also referred to as residual currents) of order $20 \, \text{cm s}^{-1}$ along the length of sandbanks. Huthnance advanced a theory for the circulation around sandbanks, and attributed it to two different forcing processes. Namely, a Coriolis effect and a frictional effect. The net effect is additive and interestingly, under appropriate conditions, the induced circulations can be in opposite directions.

This piece of work appears to have been largely picked up by sediment dynamicists (Dyer 1986), but also presents contemporary challenges for wide-area shelf sea models. The aim of this article is to interpret the original work in a way that might engage with a broader readership; discuss its relevance for the UK shelf seas; and present the implications and

---

*Email: jelt@noc.ac.uk
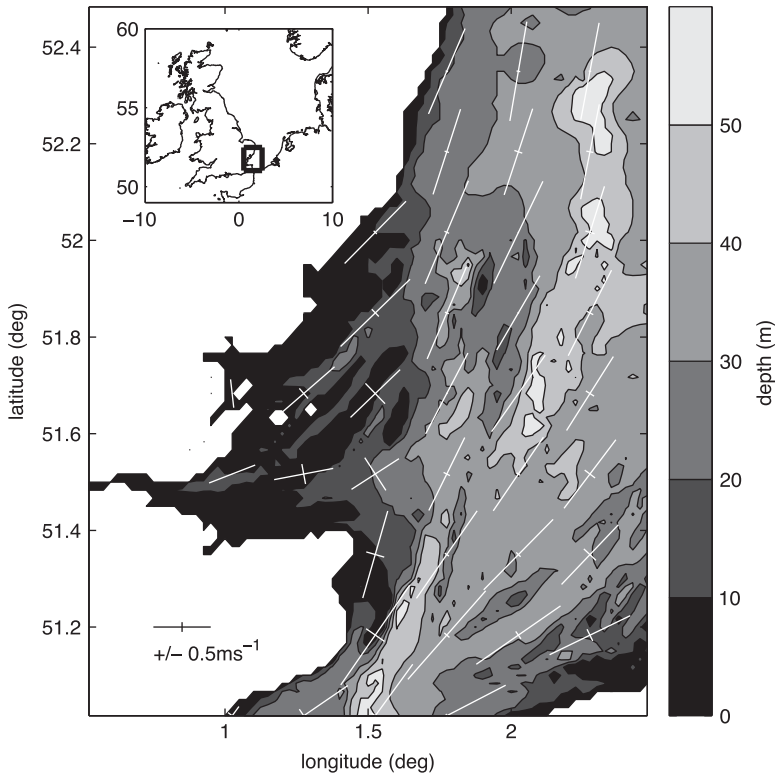
Figure 1.   Bathymetric map in the southern North Sea near the Norfolk coast, UK (Verlan and Proctor 2004). Significant sandbank features are visible that almost reach the surface. White cross-hairs denote the major and minor axes of the M2 semi-diurnal tide (subsampled from a POLCOMS HRCS simulation, Holt and Proctor 2008). The major axes of the tide do not align with the long axis of the sandbank such that there is oscillatory flow up and down the sandbank.

challenges associated with numerical simulation. As a consequence of broadening the appeal of the Huthnance (1973), approximations necessarily are made. The reader is referred to the original manuscript for a precise treatment of the problem.

In section 2, the principle mechanisms are discussed. Estimates of the tidal residual are computed in section 3. A discussion follows in section 4.

2. Mechanistic description of the tidally induced flow

In this section, a simplified interpretation is given to explain how the oscillatory flow can induce a mean flow along isobaths. The interpretation attributes the net circulation to two processes: (1) Coriolis effects and (2) inertia or frictional effects. These are investigated in turn.

2.1. *Coriolis effect*

The first effect analysed in Huthnance (1973) that induces a mean circulation under the action of oscillating tides over a variable bathymetry is interpreted as a result of the rotation of the

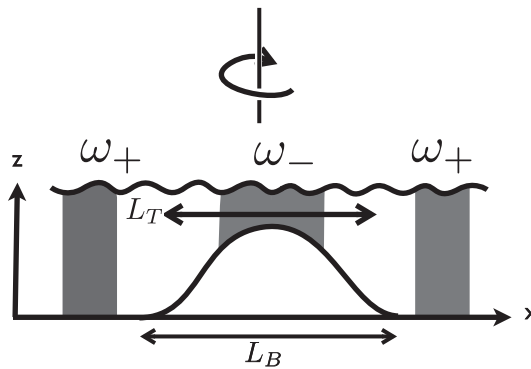Figure 2. Water that is advected off (onto) the ridge acquires a positive (negative) relative vorticity through potential vorticity conservation. The tidally averaged effect is to induce a steady clockwise circulation around a northern hemisphere bathymetric feature. Tidal excursion L_T and bathymetric scale L_B are also shown.

planet. Potential vorticity, Q, is an important dynamical quantity that captures the essence of the fluid dynamics in the rotating frame and is defined as the ratio of relative, ω, and planetary vorticity, f, to the depth of the fluid, h:

$$Q = \frac{f + \omega}{h}. \tag{1}$$

Informally, the concept of potential vorticity conservation is introduced by analogy with a spinning volume that conserves both its angular momentum and its mass. In the ocean, if a water column is stretched (squashed) by advection off (onto) a bathymetric feature, then, in order to conserve its potential vorticity, it would acquire (lose) relative vorticity. In the northern hemisphere, the net effect of an oscillatory flow of this type is to induce a negative vorticity anomaly over the bathymetric feature. A negative vorticity anomaly is associated with a clockwise circulation around the feature (figure 2).

2.2. *Inertia and frictional effects*

The interpretation of the inertia effect is based firstly on the premise that friction is relatively more important for the water column as a whole in shallower water, since fractionally more of the fluid column is within the frictional boundary layer (figure 3(a)). Thus, in deeper fluid, tidal currents generally have a surplus of momentum relative to the shallower fluid. In a rapidly adjusting fluid, the across-ridge component then advects the deep along-ridge "surplus" on-ridge and the shallow along-ridge "deficit" off-ridge (figure 3(b)). The net effect, over a tidal cycle, is to flux a mean along-ridge momentum onto the slope of the ridge. The sign, or direction, of this mean flow is determined by the along-ridge direction of the tidal current in the on-ridge phase (figure 3(c)).

This frictionally controlled mechanism was further discussed and extended to consider the effects not just of bottom friction but also lateral friction at the coastline (Zimmerman 1981).

Shown in figure 4, tidal flow parallel to frictional sea boundaries induces relative vorticity with a sign that alternates with the ebb and flood tide. In addition, if the magnitude of the tidal current varies in the along-shore direction, through, for example, an increasing damping effect of friction in a shallowing estuary, then the magnitude of the induced vorticity will similarly
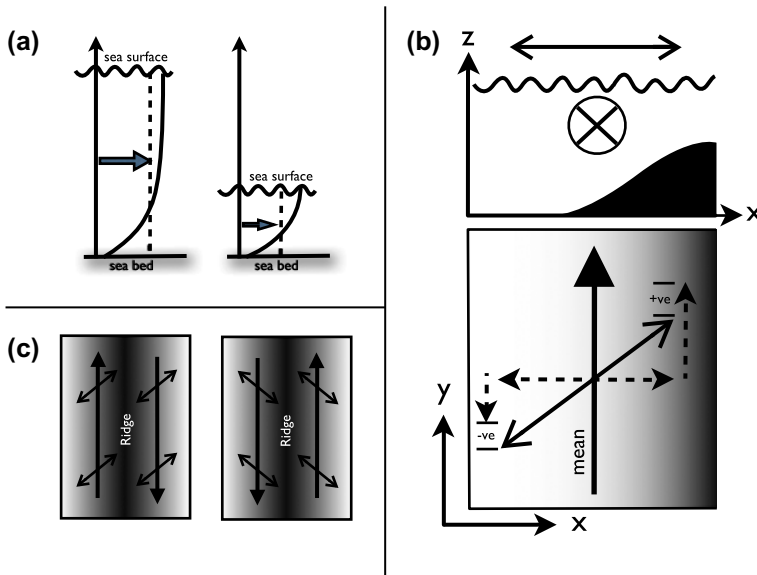
Figure 3.   Schematic highlighting that the frictional influence on a tidal current increases with reduced depth. (a) In shallow water, the damping effect of bed friction is fractionally more important. (b) A tidal flow can be decomposed into an along- and an across-ridge component. Owing to the frictionally controlled variation in tidal amplitude, a "surplus" of along-ridge momentum is advected on-ridge and a "deficit" is advected off-ridge. (c) The direction of the along-ridge mean flow is given by the direction of the along-ridge velocity in the on-ridge phase of the tide.

vary in the along-shore direction. The tidally averaged vorticity at any point in the domain will be biased towards the larger of the ebb or flood component, which will correspond to the flow from the deeper part of the domain. In an idealised shoaling estuary, this will correspond to the flood phase of the tide, as the estuary fills and the induced vorticity will correspond to a flushing circulation that leaves the estuary along the coastlines. Similarly, protruding headlands can induce anomalously large frictional vorticity responses to the ebb and flooding tides. The headland plays an equivalent role to the shoaling estuary by introducing spatial variability in the magnitude of induced vorticity in the along-coast direction. This will bias the tidally averaged vorticity in the neighbourhood of the headland and correspond to a circulation with a near coastline component that converges at the headland (figure 5).

3. Application to UK shelf seas

It is reasonable to ask how important tidal rectification of shelf sea currents is for the UK shelf seas and to make an assessment of whether or not they are simulated in shelf wide-area models. In this section, an estimate for the residual circulation is inferred from maps of the M2 tidal excursion (being the most energetic tidal constituent) and bathymetry. In particular, the tidal range map is derived from tidal velocities u_{M2} from the 3D shelf-wide hydrodynamic POLCOMS, at 1.8 km resolution, (Holt and Proctor 2008) using bathymetry from NOOS (Verlan and Proctor 2004). Then, a point-wise estimate of the tidally induced mean flows is made by considering the mean effect of vortex stretching of water columns as they are advected
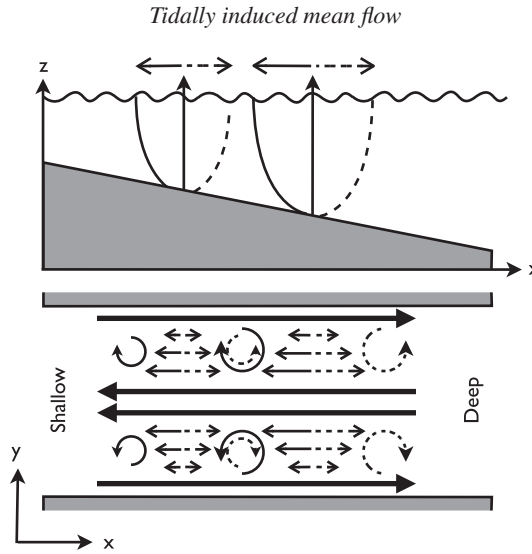
Figure 4. Schematic highlighting how the frictional influence of the coastline can induce a flushing circulation in a shoaling estuary. The ebb and flood phases are shown as dashed and solid lines. The depth controls the magnitude of the oscillating tide. The presence of frictional coastlines induces vorticity of alternating sign. Tidally averaged vorticity at a point is biased by the sign of the vorticity advected from deeper water. The corresponding mean circulation enters the channel along the axis and exits near the coast.
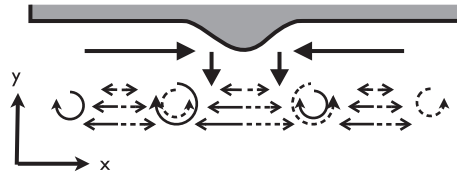

Figure 5. Schematic highlighting how the frictional influence of a coastal headland can induce a converging flow. The ebb and flood phases are shown as dashed and solid lines. The headland enhances the magnitude of tidally induced vorticity. Tidally averaged vorticity at a point is biased by the sign of the vorticity advected from near the headland. The corresponding mean flow along the coast converges at the headland.

back and forth across variable bathymetry, h, with a tidal period, T. There are two horizontal length scales in this physical problem. The scale of the bathymetry,

$$L_B = \frac{h}{|\nabla h|}, \tag{2}$$

and the scale of the tidal excursion (for M2 tidal velocity $\boldsymbol{u}_{M2}$),

$$L_T = \max_{t_0} \left| \int_{t_0}^{t_0+T/2} \boldsymbol{u}_{M2} \, \mathrm{d}t \right|, \tag{3}$$

which is twice the amplitude of the lateral tidal displacement. These are shown in figures 6(a) and (b). The degree to which these scales are numerically resolved will impact a simulation's ability to capture tidally rectified flows. Clearly, a numerical resolution that adequately resolves the smaller of L_T and L_B would suffice, but it would also be computationally very demanding. Zimmerman (1981) considered this problem and reasoned that the strongest tidally induced flows will occur when the bathymetric and tidal excursion length scales are comparable. Since,
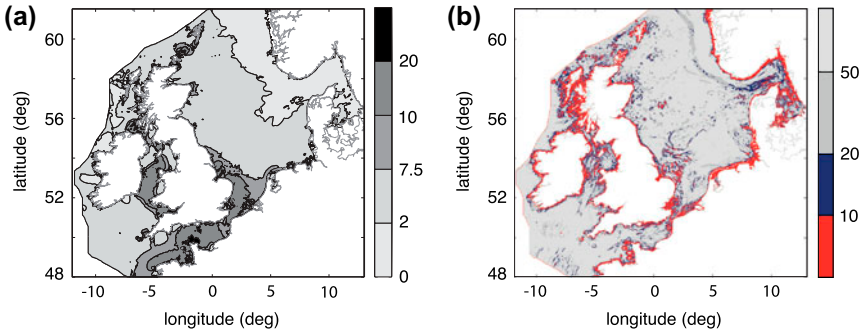
Figure 6.   (a) M2 tidal excursion L_T (km); (b) bathymetric length scale, $L_B = h/|\nabla h|$ (km).

when $L_T >> L_B$, the vortex compression and stretching processes will not be strongly correlated to the phase of the tide, resulting in a diminished time mean effect. Conversely, if $L_T << L_B$, then the water column will not significantly feel variable bathymetry over a tidal cycle.

Following Robinson (1981), a point-wise estimate for the magnitude of the induced current is given by

$$U = \alpha L_T \left(f \, \frac{\Delta h}{h} \right), \qquad \text{where} \quad \alpha = \begin{cases} 0.15 & \text{for } L_T < L_B, \\ 0 & \text{for } L_T > L_B, \end{cases} \tag{4}$$

where f is the Coriolis parameter, $\Delta h/h$ is the maximum fractional change in water depth within a tidal period and α is tuned to capture frictional effects for the case $L_T < L_B$ (Robinson 1981) or to turn the process off for $L_B < L_T$ (which would otherwise give unbounded values as $L_B \to 0$).

The maximal fractional change in water depth is given by the ratio of upslope tidal excursion $L_T^\perp$ and L_B. Algebraically, $L_T^\perp$ is defined similarly to L_T, as a point-wise tidal excursion, but it is projected onto the upslope direction $\widehat{\nabla h}$, giving $L_T^\perp = \max_{t_0} \left\{ \int_{t_0}^{t_0+T/2} \widehat{\nabla h} \cdot \boldsymbol{u}_{M2} \, dt \right\}$. Therefore,

$$\frac{\Delta h}{h} = \frac{L_T^\perp}{L_B}. \tag{5}$$

Figures 7 and 8 highlight that there are a significant number of the locations around the northwest European shelf seas that are predicted to have tidal mean flows in excess of $2\,\text{cm s}^{-1}$, and in some locations $5\,\text{cm s}^{-1}$. These are mostly coastal locations (including the southern North Sea which motivated the original Huthnance paper), but there are open-sea locations too, such as in the Celtic Sea, where there are significant submarine bathymetric features approaching the shelf break and would be expected to scale with the spring-neap phase. These persistent currents, especially near the coastlines and shelf break, could have a significant impact on biogeochemical pathways within shelf seas as well as persistent exchange channels between the shelf seas and open ocean.

Comparison of U (figure 7) with L_T and L_B highlights that elevated values of U qualitatively coincide with relatively long tidal excursions (figure 6(a)) and relatively short bathymetric length scales (figure 6(b)). The largest residual currents, O($0.05\,\text{m s}^{-1}$), occur at a matching length scale, $L_T = L_B = 10\,\text{km}$ (figure 8). Prevalence peaks, however, in smaller amplitudes
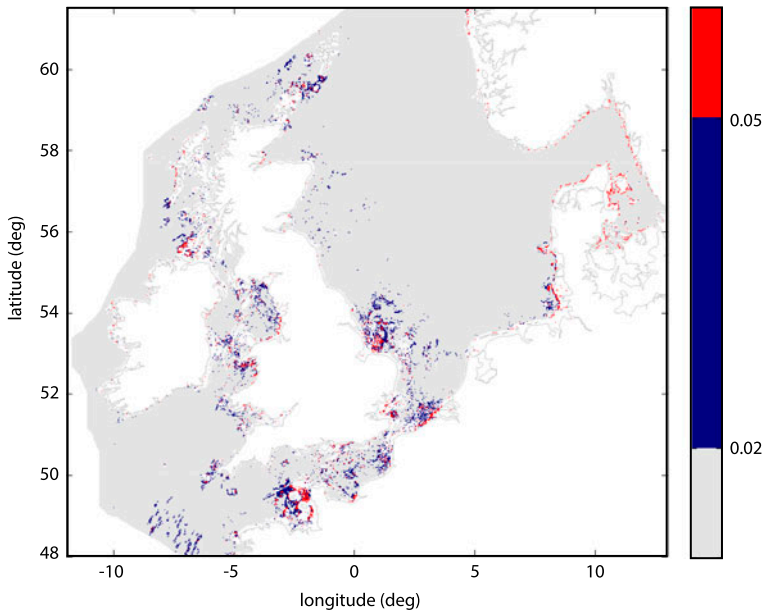
Figure 7. Estimate of persistent current speeds U induced by tidal flow over realistic bathymetry (m s^{-1}).

of residual current, e.g. $U = 0.03$ m s^{-1} occur at separated length scales with L_T shifted to shorter scales (5 km $< L_T <$ 7.5 km) and L_B shifted to longer scales ($L_B >$ 10 km).

Though equation (4) does not capture the potential for neighbouring locations to connect via a residual current, nor does it has a dynamic representation of the frictional effects that may enhance or diminish the induced mean currents, it does give a first-order estimate of the tidally induced persistent currents. Furthermore, it highlights that tidal excursions of order 5–10 km must be resolved for effective simulations at the peak in the probability density function for $U > 0.02$ m s^{-1}.

4. Discussion

Huthnance (1973) develops two additive processes for inducing mean currents from oscillating flow over variable bathymetry: a Coriolis (vortex stretching) and an inertia / frictional effect. The Coriolis effect is estimated for the north-west European shelf sea. It is found that there are a number of regions where mean flows are of order 0.05 m s^{-1}. Flows of this magnitude could have socio-economic relevance: acting as connectivity pathways for marine ecosystems; transporting sediments, nutrients and pollutants and enhancing shelf-edge exchange with the open ocean.

Analysis of the estimated tidally induced flow (figure 8) as a function of the length scales L_T and L_B supports the hypothesis that U is maximal when the L_T and L_B are comparable, but also that the dominant length scale is relatively short ($L_T \sim 5 - 7.5$ km) for more modest but prevalent residual flow estimates. A 1.8 km resolution model, for example (Holt and Proctor 2008), or the new Met Office led UK Environmental Prediction system (which will resolve the shelf seas at 1.5 km) would capture this limiting tidal excursion length scale and would,
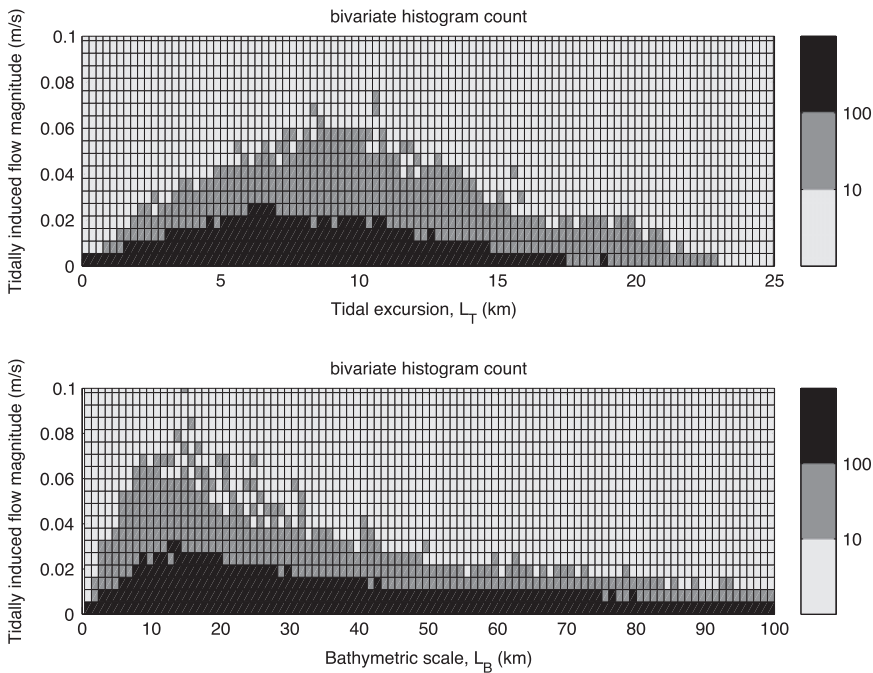
Figure 8. U plotted as a histogram against L_T and L_B. The most frequent occurrences of $U > 0.02\,\mathrm{m\,s^{-1}}$ are captured by the ranges $5 < L_T < 10\,\mathrm{km}$ and $8 < L_B < 30\,\mathrm{km}$.

therefore, capture the largest contributions of the tidally induced flow. However, the current Met Office 7 km resolution operational model for shelf seas (O'Dea *et al.* 2012) will clearly not resolve these scales and will, therefore, poorly resolve tidally induced residual flows.

Noting the tidal residual hotspots (figure 7), it is anticipated that canyons in the south-west Celtic Sea, that extend from the shelf break onto the shelf, could act as important channels for persistent exchange of water masses. Similarly, tidal residual flows could be important for flushing freshwater and its solute load out of coastal areas around The Wash in south-east England or it could determine the flushing timescales of the Irish Sea through the North Channel.

No estimate has been made here to quantify the effect of stratification on the tidal residual, though the candidate hotspots suggested in figure 7 correspond to permanently mixed regions of the shelf sea, that are well predicted by the h/u^3 Simpson and Hunter (1974) mixing parameter (with the notable exception of the Celtic Sea, which is seasonally stratified).

In order to assess the connectivity issues arising from tidal rectification and to better include friction effects, Lagrangian experiments must be conducted in simulations with and without tides. Work is underway as part of the NERC FASTNEt programme to build a 1.8 km model that spans the entire shelf and shelf break and with which these questions, and others, can be investigated.

Acknowledgements

a broad range of specialisms. Of course, figuring out what are the important problems to solve is no small part of this challenge, but I'm sure that John's involvement in observational programmes, management and policy has certainly informed him well. His example serves as a contemporary model and challenge to all. Thank you to the reviewer for their helpful comments. This work was funded under the Natural Environment Research Council (NERC) FASTNEt consortium [NE/I030259/1] and was a JCOMP scoping activity.

References

Caston, V.N.D. and Stride, A.H., Tidal sand movement between some linear sand banks in the North Sea off northeast Norfolk. *Mar. Geol.* 1970, **9**, M38–M42.

Dyer, K.R., *Coastal and Estuarine Sediment Dynamics*, 1986. (Chichester: Wiley).

Holt, J. and Proctor, R., The seasonal circulation and volume transport on the northwest European continental shelf: A fine-resolution model study. *J. Geophys. Res.* 2008, **113**, C06021, 10.1029/2006JC004034.

Huthnance, J.M., Tidal current asymmetries over the Norfolk Sandbanks. *Estuarine Coastal Mar. Sci.* 1973, **1**, 89–99.

O'Dea, E., Arnold, A., Edwards, K., Furner, R., Hyder, P., Martin, M., Siddorn, J., Storkey, D., While, J., Holt, J. and Liu, H., An operational ocean forecast system incorporating NEMO and SST data assimilation for the tidally driven European North-West shelf. *J. Oper. Oceanogr.* 2012, **5**, 3–17.

Robinson, I.S., Tidal vorticity and residual circulation. *Deep Sea Res. Part A* 1981, **28**, 195–212.

Simpson, J.H. and Hunter, J.R., Fronts in the Irish Sea. *Nature* 1974, **250**, 404–406.

Verlan, M. and Proctor, R., NOOS bathymetry 1.0, 2004. Available online at: www.noos.cc/fileadmin/user_upload/Reports/bathymetry_poster.pdf .

Zimmerman, J.T.F., Dynamics, diffusion and geomorphological significance of tidal residual eddies. *Nature* 1981, **290**, 549–555.